

Electronic Properties and Device Applications of Quasi-2D Charge-Density-Wave Materials

Alexander A. Balandin

Nano-Device Laboratory: NDL
Center for Phonon Optimized Engineered Materials: POEM
Department of Electrical and Computer Engineering
Materials Science and Engineering Program
University of California – Riverside

MRS 2020
Keynote – Live Session

Acknowledging Students



Dr. G. Liu, Apple



Dr. R. Salgado, Intel



Dr. A. Geremew, Intel



Dr. E. Aytan, Intel



Dr. S. Naghibi, Keysight Tech



Dr. F. Kargar, UCR



Z. Barani, UCR



S. Baraghani, UCR

Funding Acknowledgement

Department of Energy (DOE) contract DE-SC0021020 Physical Mechanisms and Electric-Bias Control of Phase Transitions in Quasi-2D Charge-Density-Wave Quantum Materials

UCR PI: A.A. Balandin



National Science Foundation (NSF) program Designing Materials to Revolutionize and Engineer our Future (DMREF) via a project DMR-1921958 entitled Collaborative Research: Data Driven Discovery of Synthesis Pathways and Distinguishing Electronic Phenomena of 1D van der Waals Bonded Solids

UCR PI: A.A. Balandin, Co-PI: L. Bartels; Stanford Lead PI: E. Reed



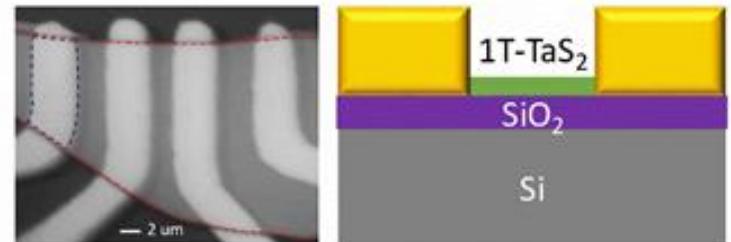
NSF DMR Major Research Instrumentation (MRI): Development of a Cryogenic Integrated Micro-Raman-Brillouin-Mandelstam Spectrometer

UCR PI: A.A. Balandin, Co-PI: F. Kargar



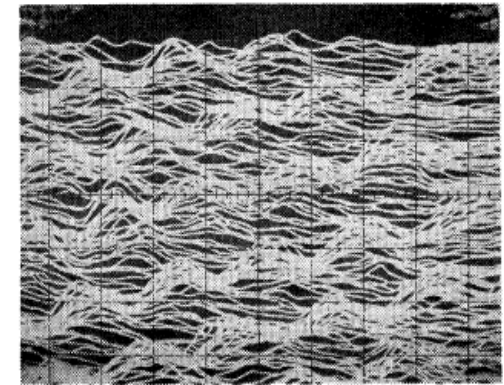
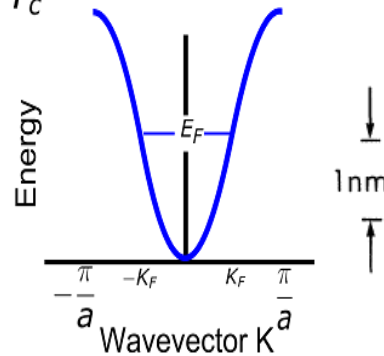
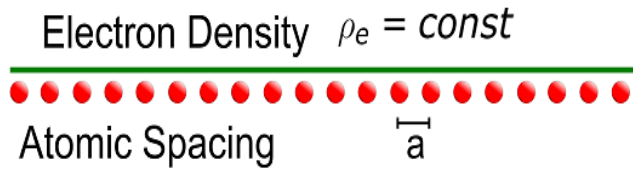
Outline of the Talk

- Quasi-2D charge-density-wave devices
 - Room temperature operation
 - The use of NC-CDW – IC-CDW transition
 - Switching all the way to metallic phase
 - Noise spectroscopy of phase transitions
- Radiation hardness
- Mechanism of switching
- The search for the “narrow band noise”
- Conclusions

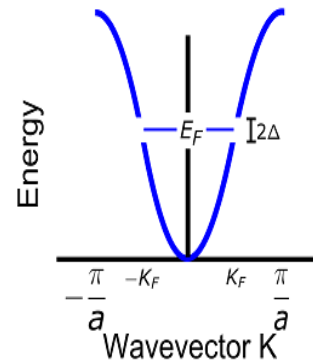
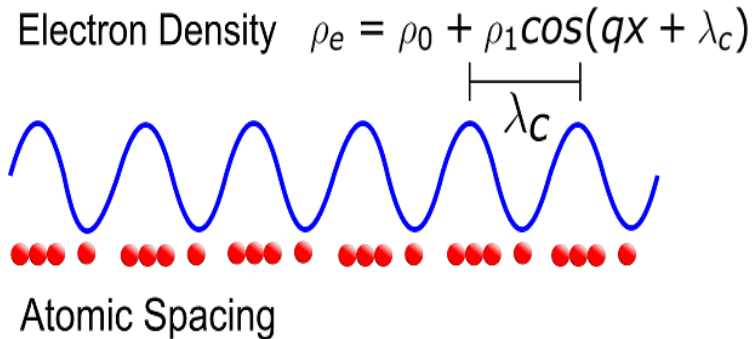


Charge Density Waves: Bulk 1D Crystals

Normal state $T > T_c$



Peierls state $T < T_c$



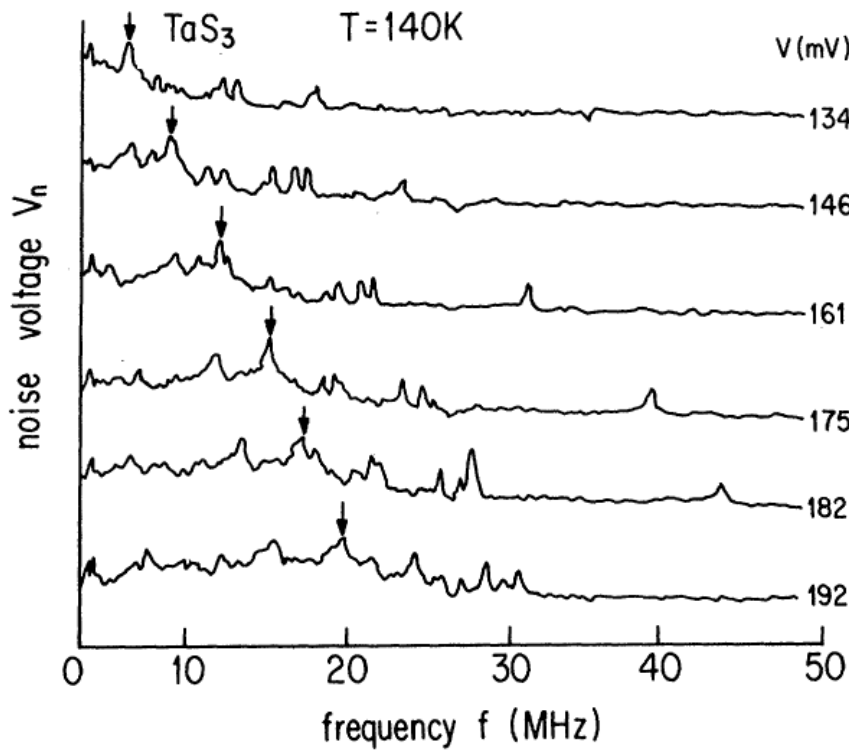
→ | 1 nm | ←

R.V. Coleman, *Phys. Rev. Lett.*, **55**, 394 (1985).

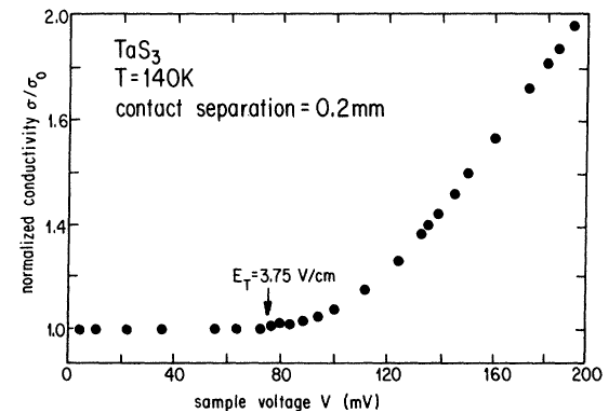
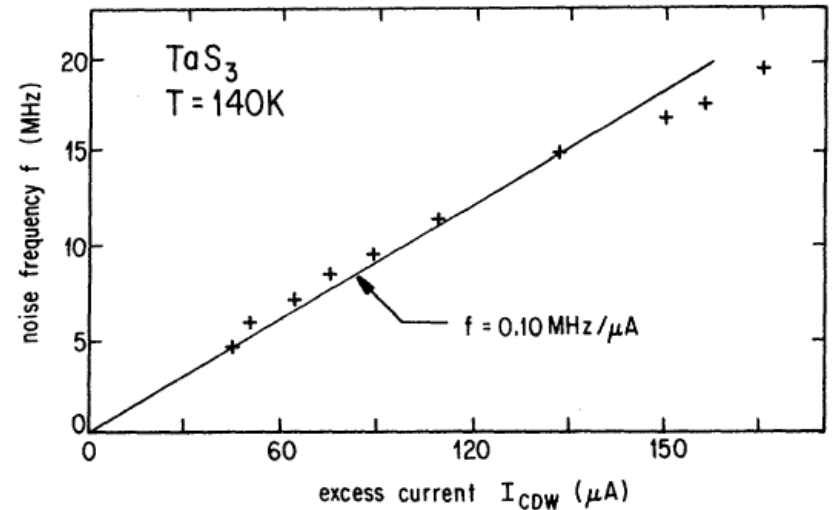
Macroscopic quantum phenomena: coherence length $> 1 \mu\text{m}$

Quantum materials

Examples of Current Oscillations in Bulk Quasi-1D CDW Materials



G. Gruner, et al., Phys. Rev. B, 23, 6813 (1981).

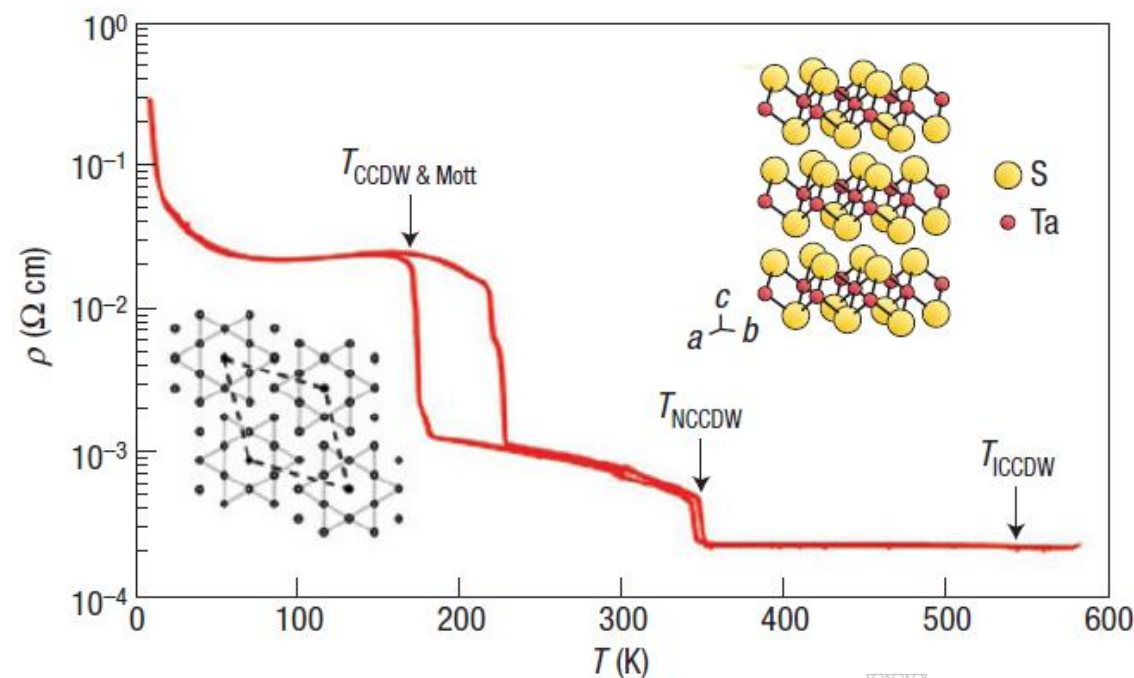


Types of CDW Phase Transitions

- There is no uniform mechanism to explain the origin of CDW in different systems, which means truly quantitative predictions of CDW properties for a new material are practically impossible.
- **Type I – CDW in 1D Peierls' model:** band-gap (or FSN) in electronic structure, Kohn anomaly in phonon spectra, a structural transition in lattice and a metal–insulator transition. **Examples:** NbS_3 ; TaS_3
- **Type II – CDW in 2D electron–phonon coupling model:** The CDW in 2D is not driven by FSN. Instead, the CDW phases are dictated by the q-dependent electron–phonon coupling (EPC). **Examples:** NbSe_2 ; TaSe_2 ; TaS_2
- **Type III – CDW with 3D character:** charge modulation or charge ordering with no indication of FSN or EPC as the driving force. **Examples:** rare earth systems such as $\text{R}_5\text{Ir}_4\text{Si}_{10}$

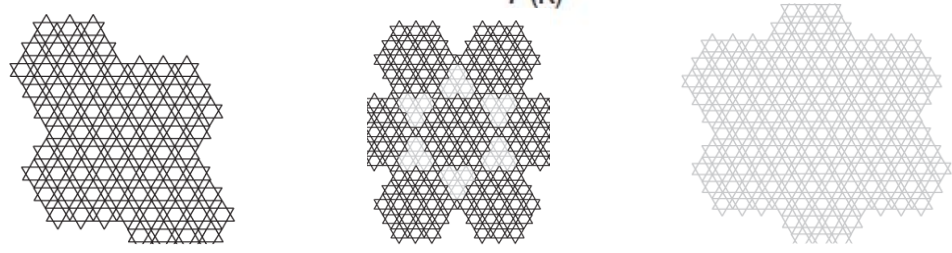
Xuetao Zhu, Jiandong Guo, Jiandi Zhang & E. W. Plummer (2017) Misconceptions associated with the origin of charge density waves, *Advances in Physics: X*, 2:3, 622-640, DOI: 10.1080/23746149.2017.1343098

Rebirth of the Field of CDW Materials: Quasi-2D Films of 1T-TaS₂



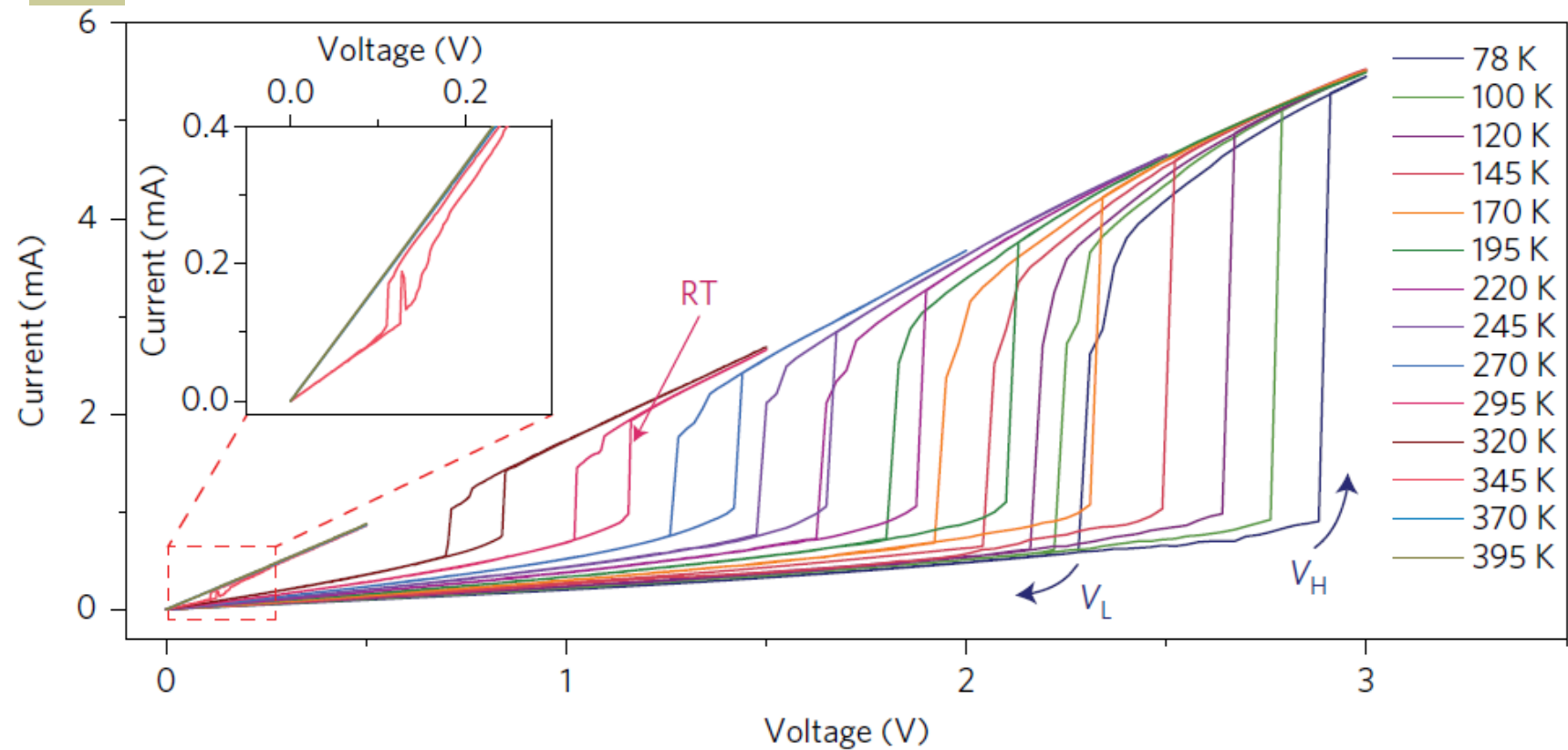
Ambient-pressure phases of 1T-TaS₂. The phases are: a metallic phase at temperatures above 550 K; an IC-CDW phase above 350 K; an NC-CDW phase above 190 K; a C-CDW Mott phase below 190 K. Also shown are the Ta atom distortions in the fully commensurate phase and the crystal structure of 1T-TaS₂.

B. Sipoš, A.F. Kusmartseva, A. Akrap, H. Berger, L. Forró, and E. Tutiš, Nature Mater., 7, 960 (2008).



There are multiple phase transition points – some of them are above RT

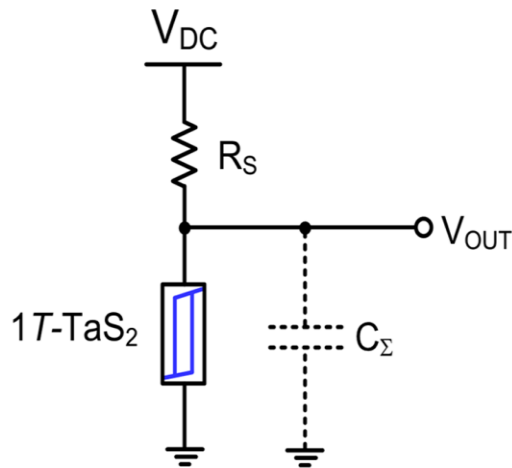
I-V Characteristics of Thin Film 1T-TaS₂



The threshold switching effect is prominent from 78 K to 320 K. The blue arrows indicate the voltage sweep direction for the measurement at 78 K. For all the other temperatures, V_H is always higher than V_L. The switching is prominent up to 320 K, and becomes less pronounced as the temperature approaches the NC-CDW-IC-CDW transition at 350 K. As shown in the inset, at 345 K (red curve), the switching is still measurable.

G. Liu, B. Debnath, T. T. Salguero, R. K. Lake, and A. A. Balandin, *Nature Nano*, 11, 845 (2016).

First Room-Temperature CDW Device

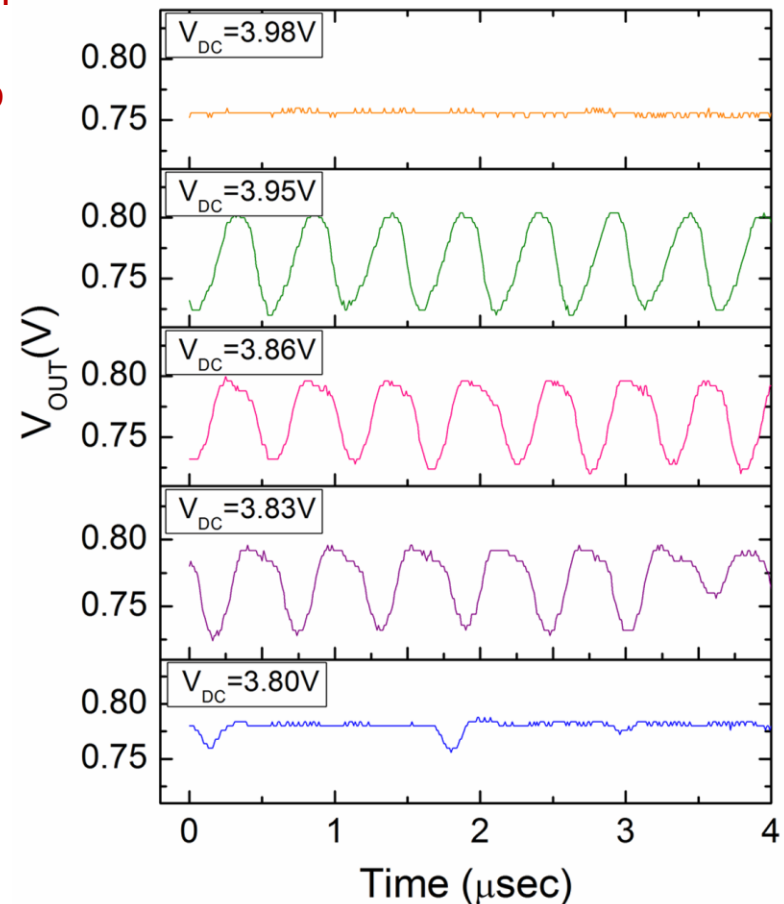


Different operation mechanism from early devices – no de-pinning

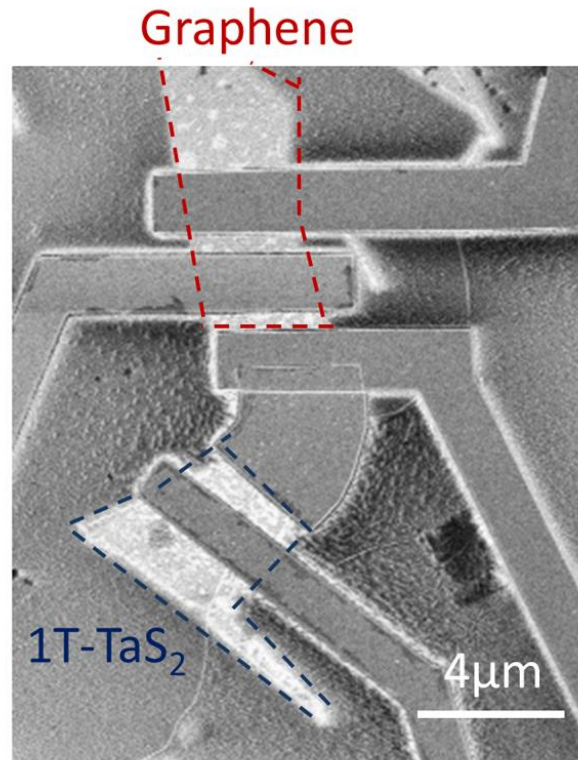
Allows for high T operation

→ Circuit schematic of the oscillator consists of the 1T-TaS₂ film, a series connected load resistor, and a lumped capacitance from the output node to ground. The load resistance is 1 kΩ.

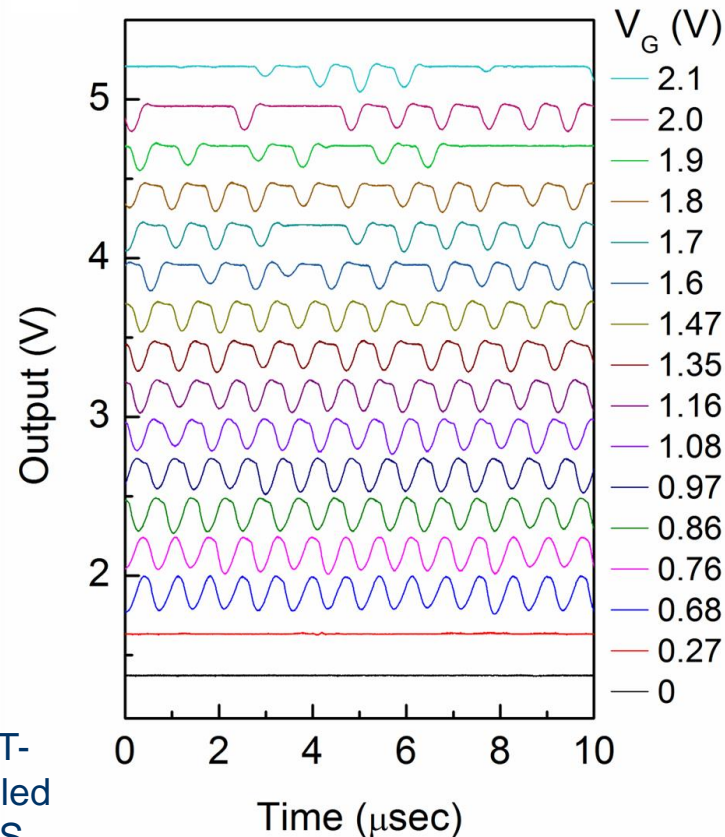
→ Voltage oscillations under different V_{DC} . The circuit oscillates when V_{DC} is within the range of 3.83-3.95 V. The frequency is 1.77 MHz, 1.85 MHz, and 2 MHz when V_{DC} is 3.83, 3.86 and 3.95 V, respectively.



Integrated 1T-TaS₂ – h-BN – Graphene VCO



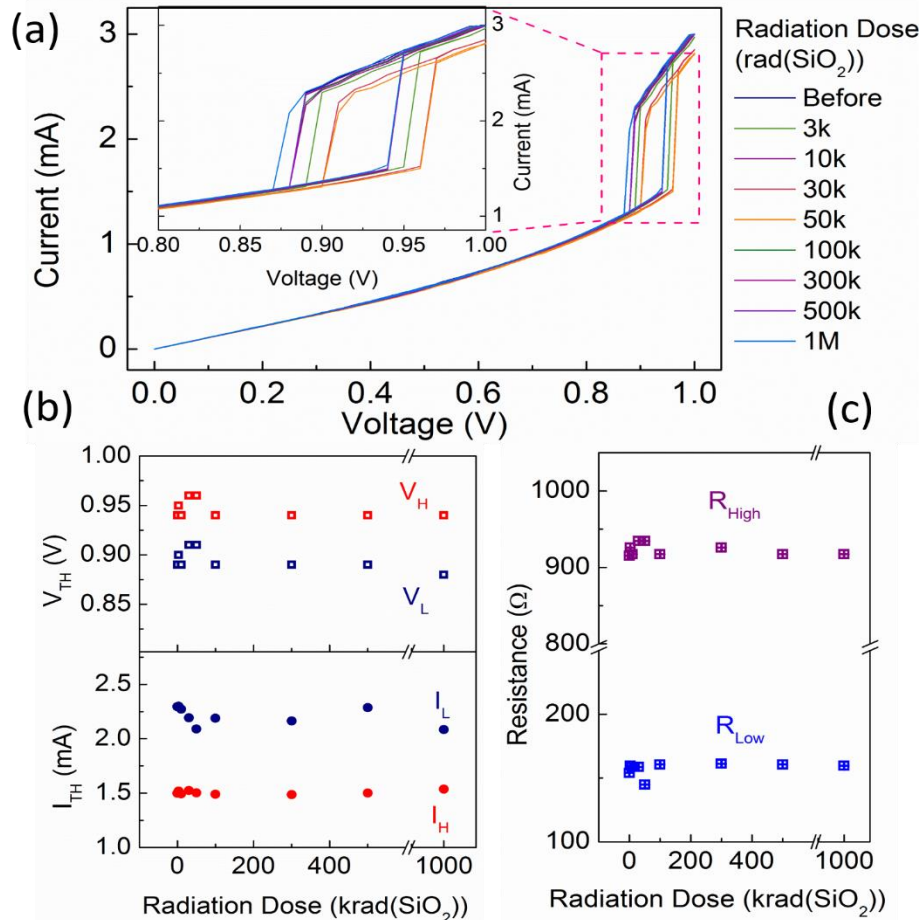
The SEM image of the integrated 1T-TaS₂-BN-graphene voltage controlled oscillator. The graphene and the TaS₂ are highlighted by dashed lines.



Output waveforms at different gate biases when V_{DC} is fixed at 3.65 V. The oscillation frequency is tunable with gate biases in the range of 0.68 V to 1.8 V. The different waveforms are vertically offset of 0.25 V for clarity.

G. Liu, B. Debnath, T. T. Salguero, R. K. Lake, and A. A. Balandin, Nature Nano, 11, 845 (2016).

1T-TaS₂ CDW Devices Under X-Ray Irradiation

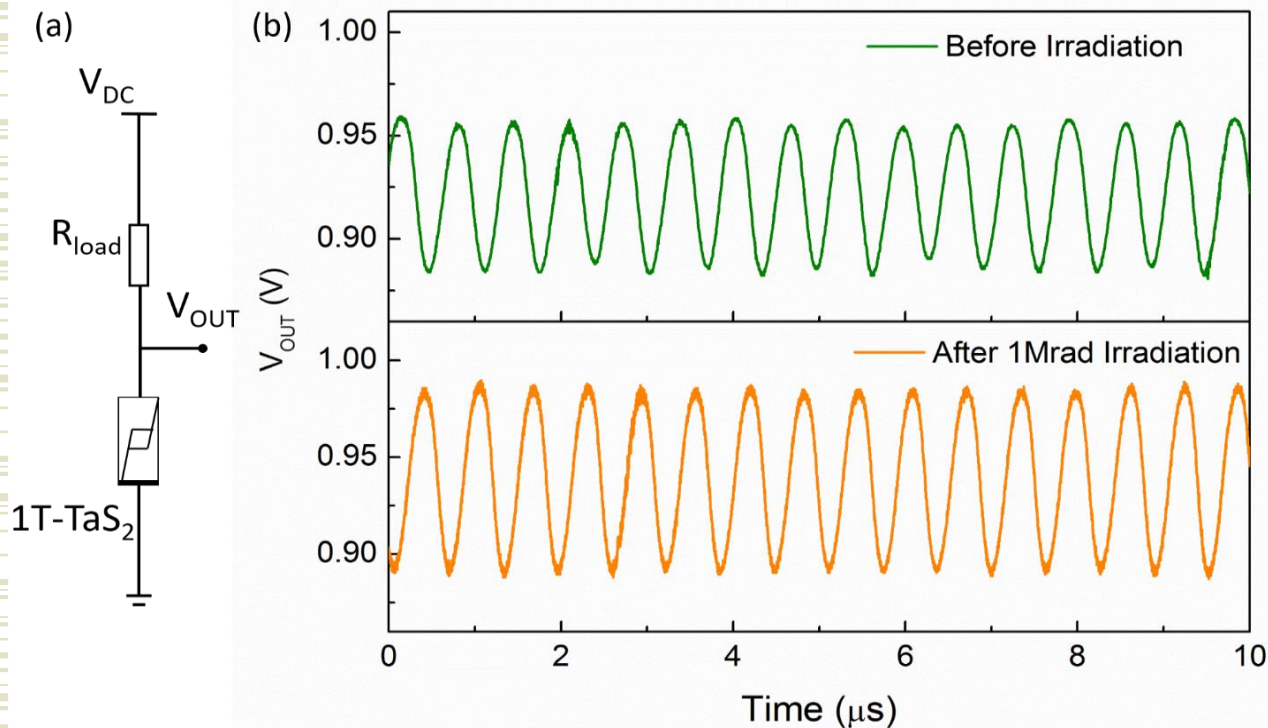


TID response of 1T-TaS₂ devices up to 1 M rad (SiO₂). (a) I-V curves measured after each X-ray irradiation step. (b) Threshold voltages, V_H and V_L , threshold currents, I_H and I_L as function of dose. (c) Extracted resistance at the high resistance and low resistance states as a function of dose.

Carrier concentration:
 $10^{21} \text{ cm}^{-2} - 10^{22} \text{ cm}^{-2}$

G. Liu, E. X. Zhang, C. Liang, M. Bloodgood, T. Salguero, D. Fleetwood, A. A. Balandin, "Total-ionizing-dose effects on threshold switching in 1T-TaS₂ charge density wave devices," IEEE Electron Device Letters, 38, 1724 (2017).

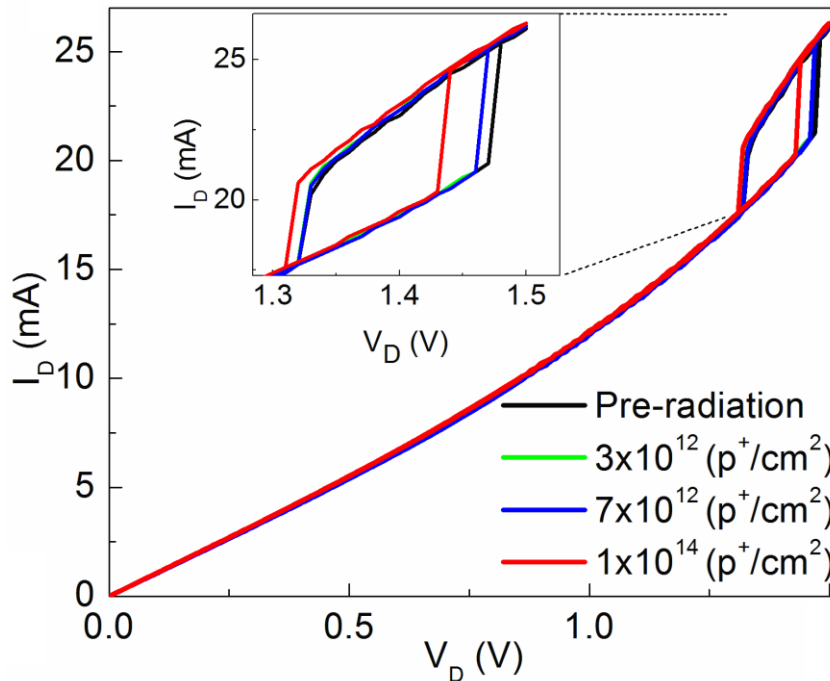
Radiation Hardness of CDW Devices



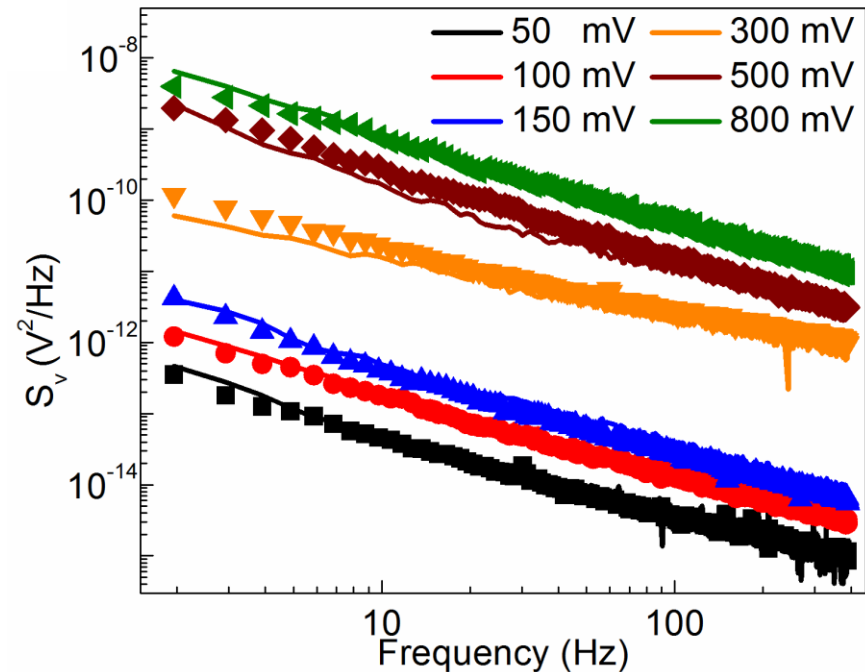
- (a) Circuit schematic diagram of a self-sustaining oscillator implemented with one 1T-TaS₂ device and a load resistor.
- (a) Oscillation waveform before and after 1 Mrad(SiO₂) X-ray irradiation

G. Liu, E. X. Zhang, C. Liang, M. Bloodgood, T. Salguero, D. Fleetwood, A. A. Balandin, "Total-ionizing-dose effects on threshold switching in 1T-TaS₂ charge density wave devices," IEEE Electron Device Letters, 38, 1724 (2017).

Proton Bombardment Immune Devices Based on CDW Transition in 1T-TaS₂



The quasi-two-dimensional (2D) 1T-TaS₂ channels show a *remarkable* immunity to bombardment with the high-energy 1.8 MeV protons to, at least, the irradiation fluence of 10^{14} H⁺cm⁻².

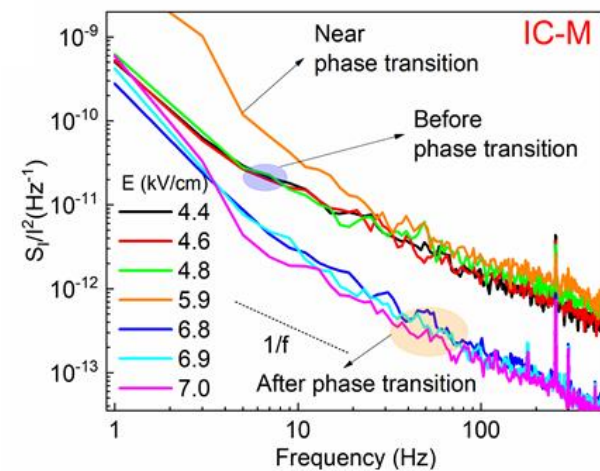
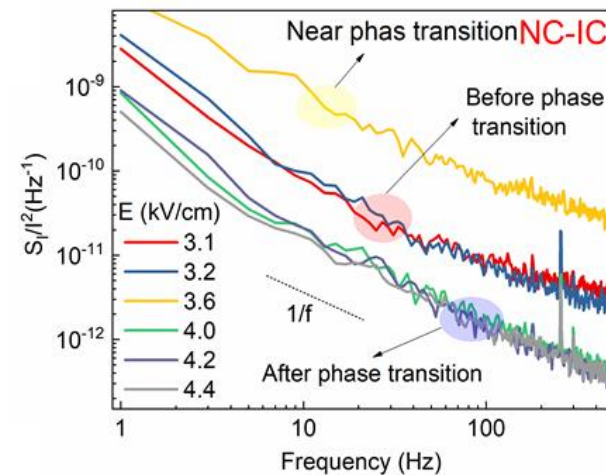


A. K. Geremew, F. Kargar, E. X. Zhang, S. E. Zhao, E. Aytan, M. A. Bloodgood, T. T. Salguero, S. Rumyantsev, A. Fedoseyev, D. M. Fleetwood and A. A. Balandin, *Nanoscale*, 11, 8380 (2019).

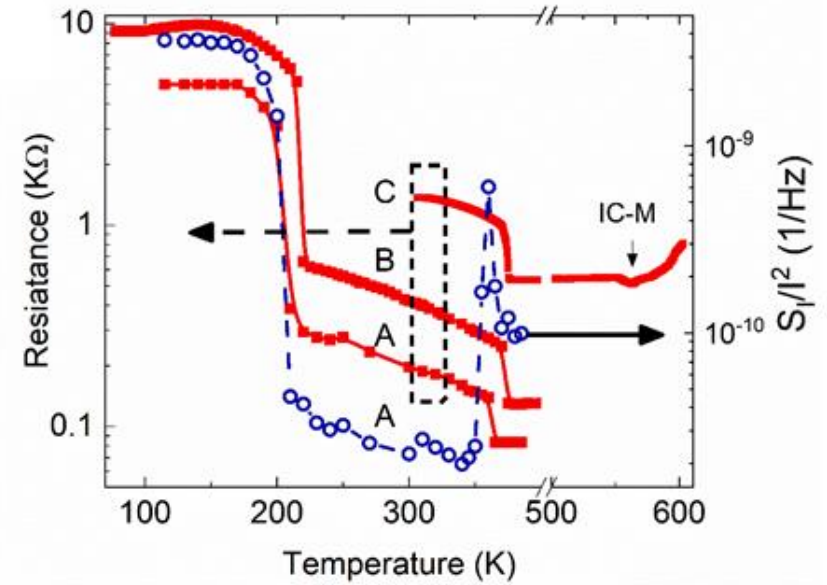
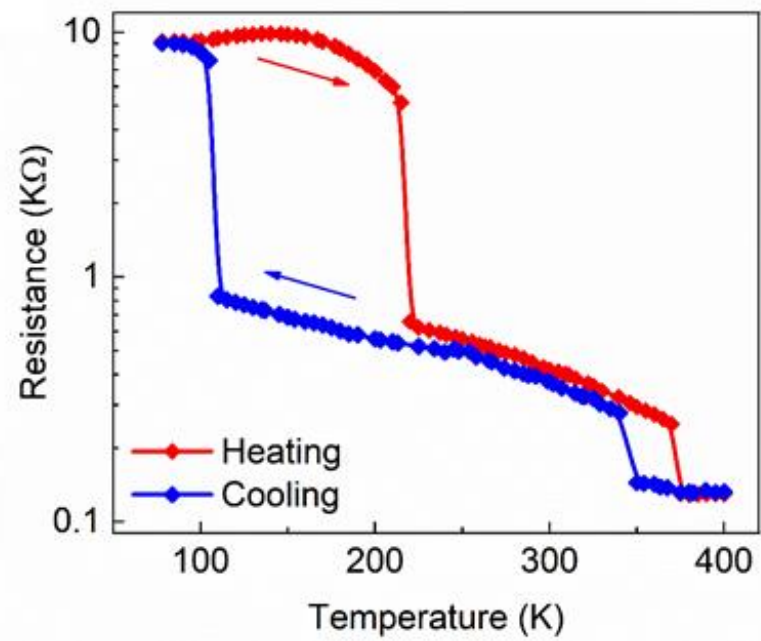
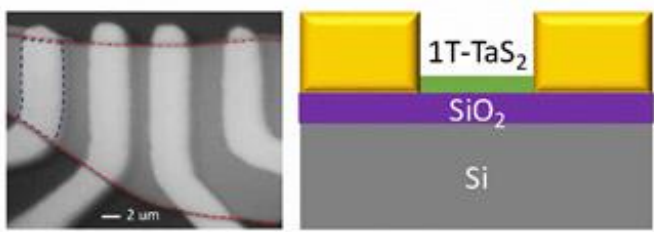
Noise Spectroscopy of CDW Phases



- G. Liu, et al., "Low-frequency current fluctuations and sliding of CDWs in two-dimensional materials," Nano Letters, 18, 3630 (2018).
- A. K. Geremew, et al., "Bias-voltage driven switching of the charge-density-wave and normal metallic phases in 1T-TaS₂ thin-film devices," ACS Nano, 13, 7231 (2019).
- R. Salgado, et al., "Low-frequency noise spectroscopy of CDW phase transitions in vertical quasi-2D 1T-TaS₂ devices," Appl. Phys. Express, 12, 037001 (2019).

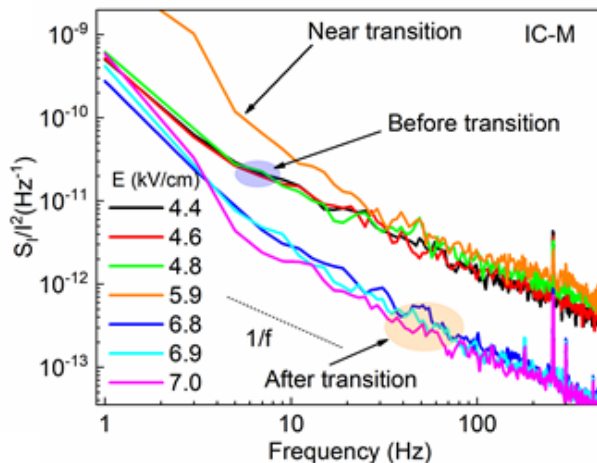
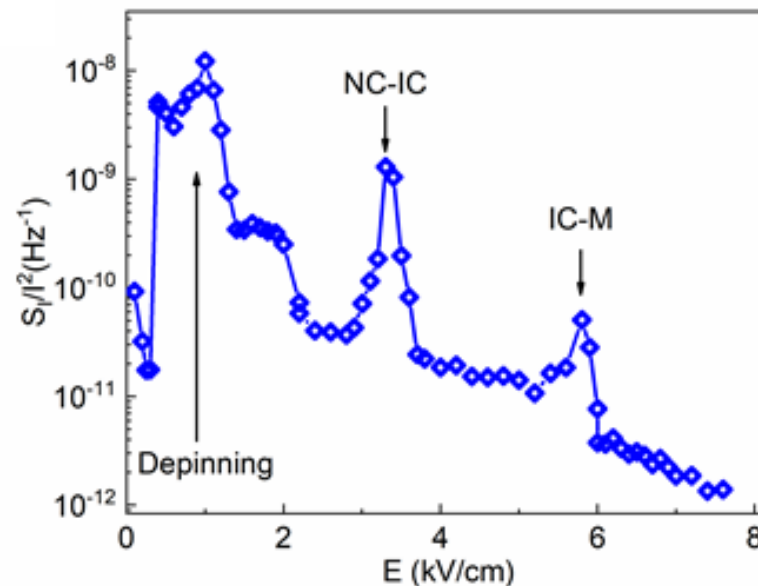
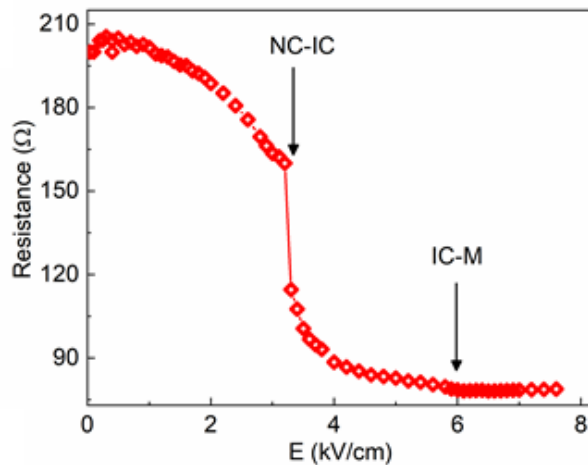


IC CDW – Metal Transition in Quasi-2D CDW Materials



- Optical image of a representative device (left panel) and a schematic of the device layered structure (right panel). The scale bar is 2 μm.
- Resistance as function of temperature for cooling (blue curve) and heating (red curve) cycles conducted at the rate of 2 K per minute.

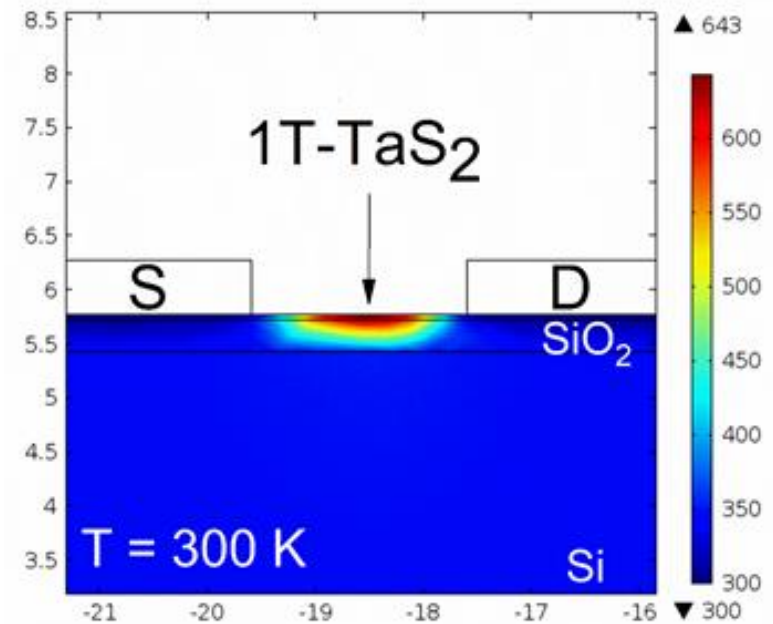
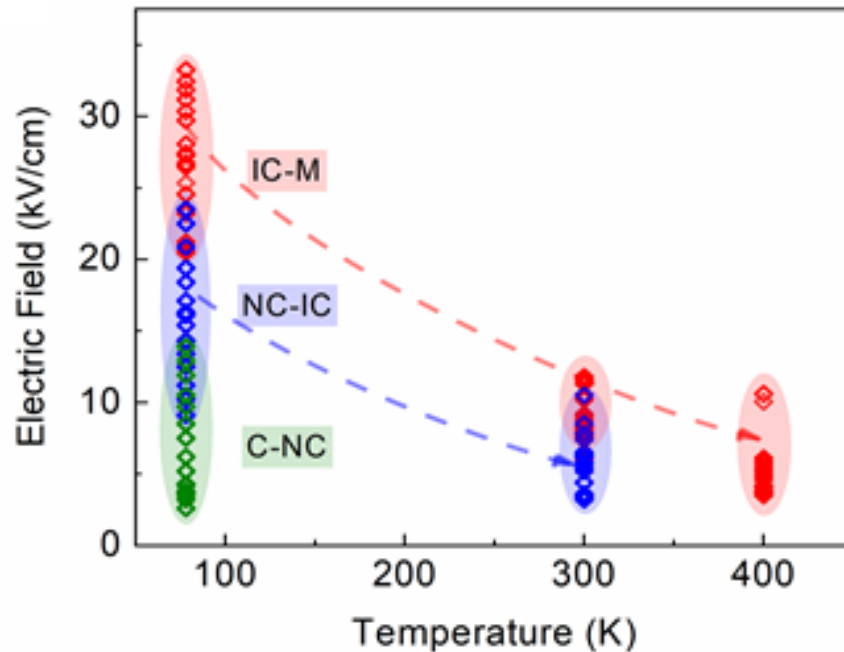
Noise Spectroscopy of CDW Transitions



- Resistance as a function of the applied electric field measured at RT.
- Noise spectral density as the function of frequency for several values of the electric field, which include the point of transition from the IC-CDW to the normal metallic phase.
- Noise spectral density, measured at $f=10$ Hz, as the function of the electric field.

A. K. Geremew, S. Rumyantsev, F. Kargar, B. Debnath, A. Nosek, M. A. Bloodgood, M. Bockrath, T. T. Salguero, R. K. Lake, and A. A. Balandin, ACS Nano, 13, 7231 (2019). 17

Electric Field vs Self-Heating Mechanism in CDW Devices

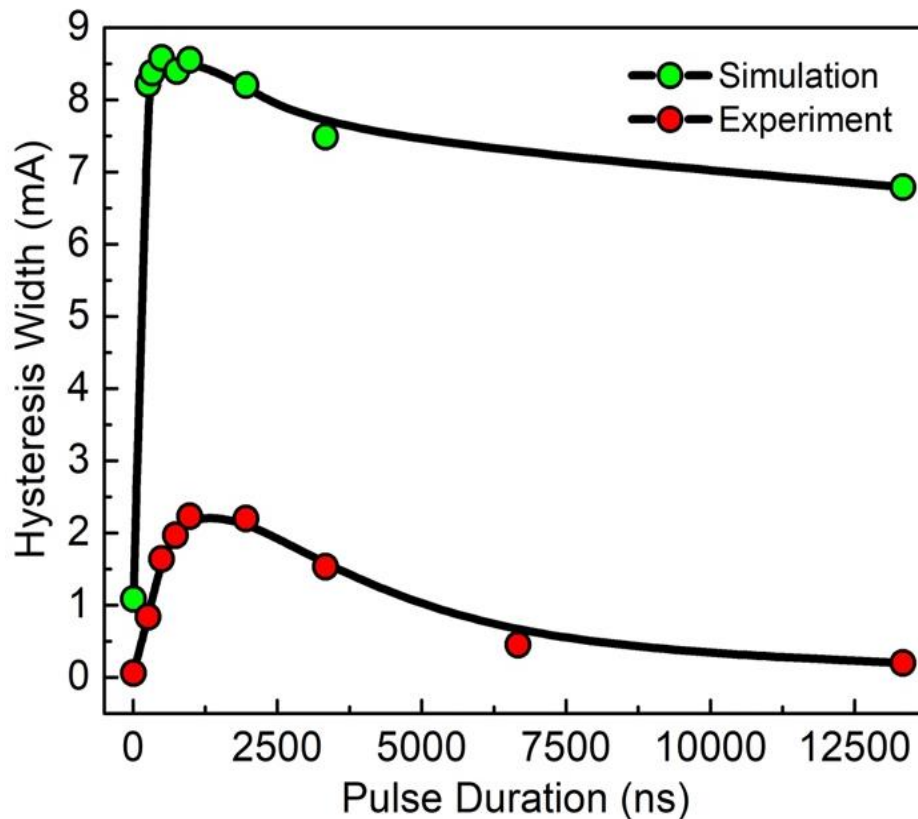


Summary of electric field induced phase transitions at different temperatures for 1T-TaS₂ devices. The variation in the electric field required to include the phase transitions is due to different device geometries, thickness of the layers in the device structures, and other variations in the device designs.

A. K. Geremew, S. Rumyantsev, F. Kargar, B. Debnath, A. Nosek, M. A. Bloodgood, M. Bockrath, T. T. Salguero, R. K. Lake, and A. A. Balandin, ACS Nano, 13, 7231 (2019).

Thermally Driven CDW Switching

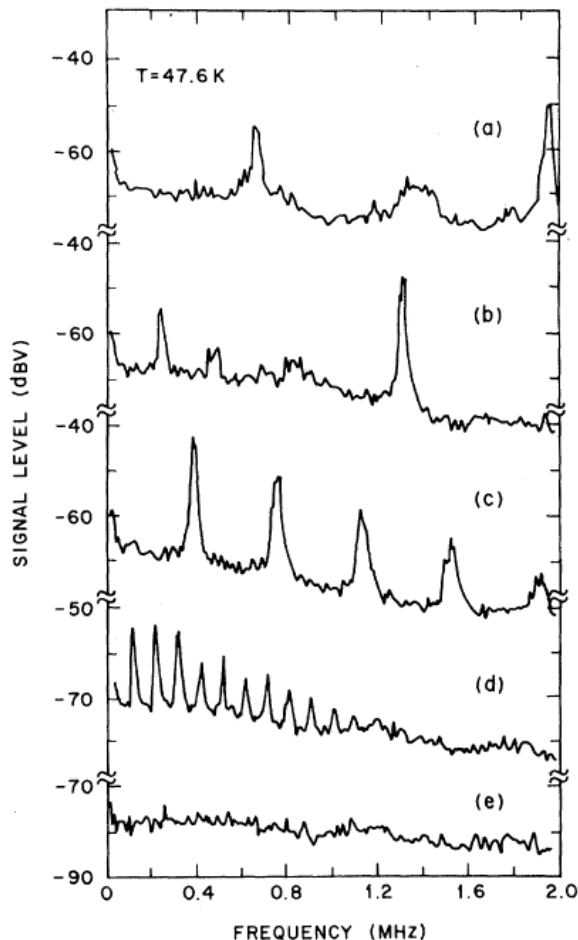
Collaboration with Professor J. P. Bird
University at Buffalo



Experimental, and simulated hysteresis window width ($I_c - I_h$) calculated at the constant bias voltage of 1 V as a function of pulse duration. The experimental and theoretical results both follow the same trend, exhibiting a peak at shorter pulse durations and saturating at longer pulse times.

Preliminary conclusion: Modeling shows that the thermally driven device can operate at GHz range.

Current Oscillations in Bulk Quasi-1D CDW Materials



Sliding-Mode Conductivity in NbSe₃: Observation of a Threshold Electric Field and Conduction Noise

R. M. Fleming and C. C. Grimes

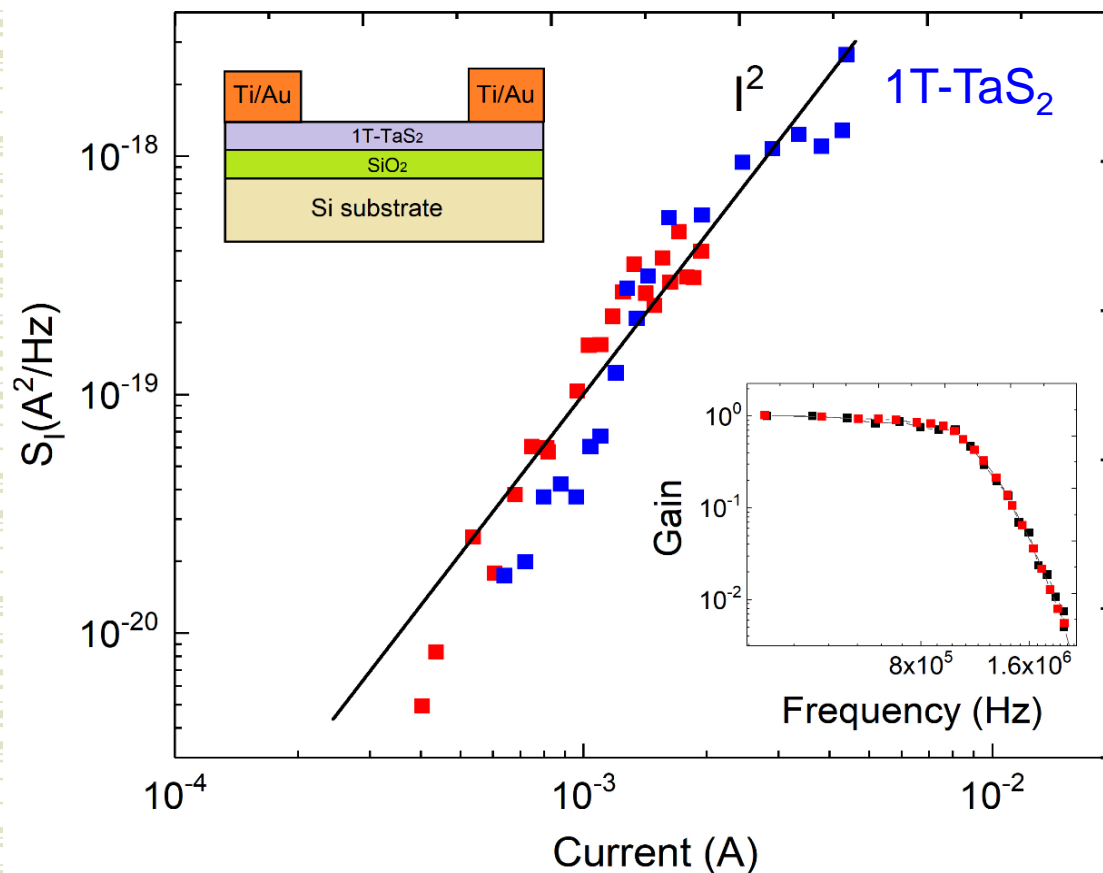
Bell Laboratories, Murray Hill, New Jersey 07974

(Received 15 March 1979)

FIG. 3. Output of on-line spectrum analyzer for selected values of current. Increasing current from zero (e) to a value above threshold (d) results in an increase of broad-band noise plus a discrete frequency with numerous harmonics. The frequency increases with current and at higher currents (b) a second frequency appears. Currents and dc voltages (a) $I = 270 \mu\text{A}$, $V = 5.81 \text{ mV}$, (b) $I = 219 \mu\text{A}$, $V = 5.05 \text{ mV}$, (c) $I = 154 \mu\text{A}$, $V = 4.07 \text{ mV}$, (d) $I = 123 \mu\text{A}$, $V = 3.40 \text{ mV}$, (e) $I = V = 0$. Sample cross section $\approx 136 \mu\text{m}^2$.

“Narrow band noise” was considered to be a direct evidence of CDW de-pinning and sliding.

The Search for the “Narrow Band Noise” in Quasi-2D CDWs

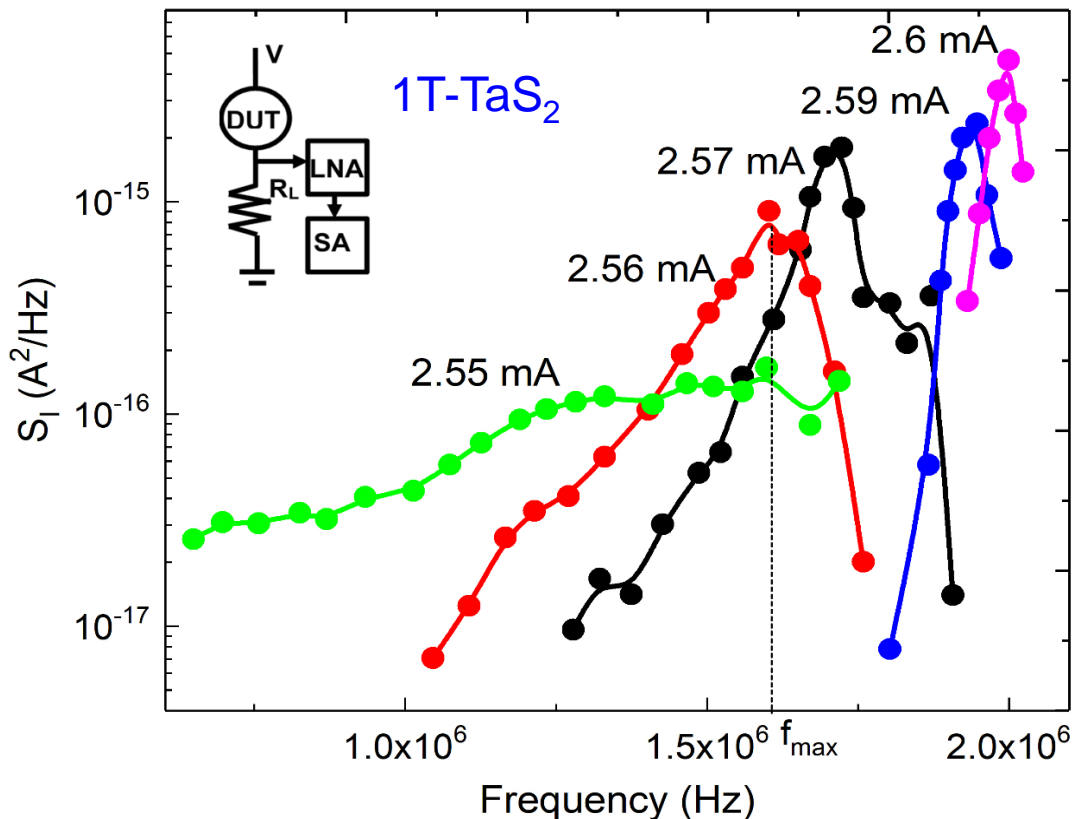


Noise power spectral density, S_I , as a function of the current through 1T-TaS₂ device channel measured at frequency $f=760$ kHz. The red and blue data points correspond to two tested devices.

The lower inset shows the gain, normalized to the gain at $f=30$ kHz, as a function of frequency.

Adane K. Geremew, Sergey Rumyantsev, Roger Lake, Alexander A. Balandin, Current Oscillations in Quasi-2D Charge-Density-Wave 1T-TaS₂ Devices: Revisiting the "Narrow Band Noise" Concept, arXiv:2003.00356 (2020)

The Signatures of the “Narrow Band Noise” in Quasi-2D CDWs

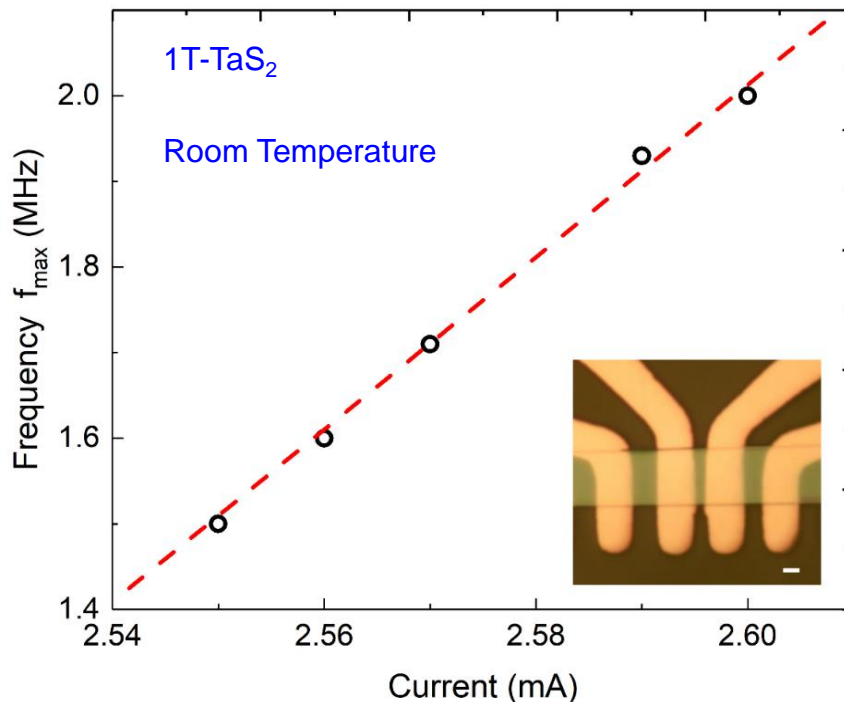


Noise as a function of frequency for several value of the current through the device channel. The peak shifts to the higher frequency f_0 with the increasing current.

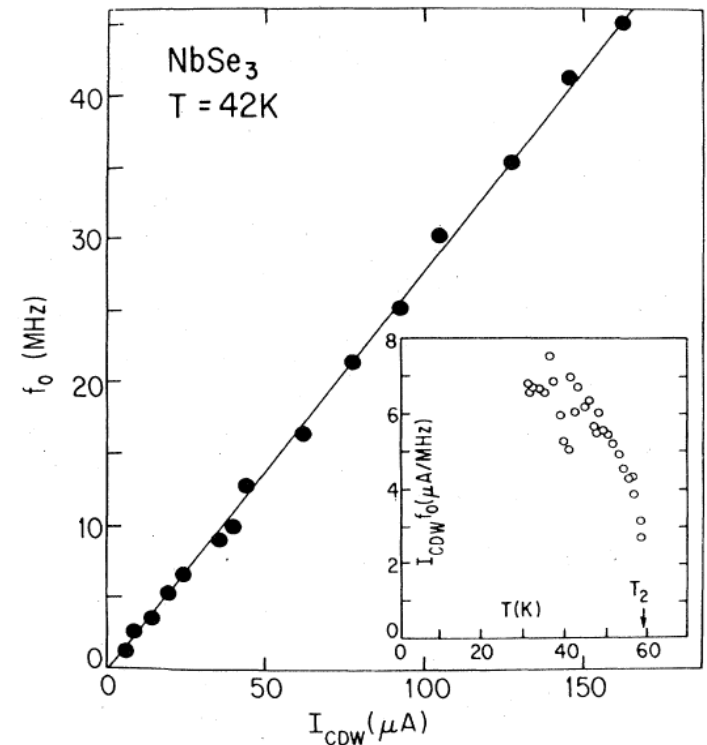
In bulk quasi-1D CDW materials, the linear relationship was explained assuming that f is proportional to the CDW drift velocity, v_D , so that $f=v_D/\Lambda$, where Λ is the characteristic distance.

Since $I_{CDW}=nef\Lambda A$, where n is the charge carrier density, e is the charge of an electron, and A is the cross-sectional area, one obtains:
 $f=(1/ne\Lambda A) \times I_{CDW}$

Have We Found the “Narrow Band Noise” in Quasi-2D CDWs?

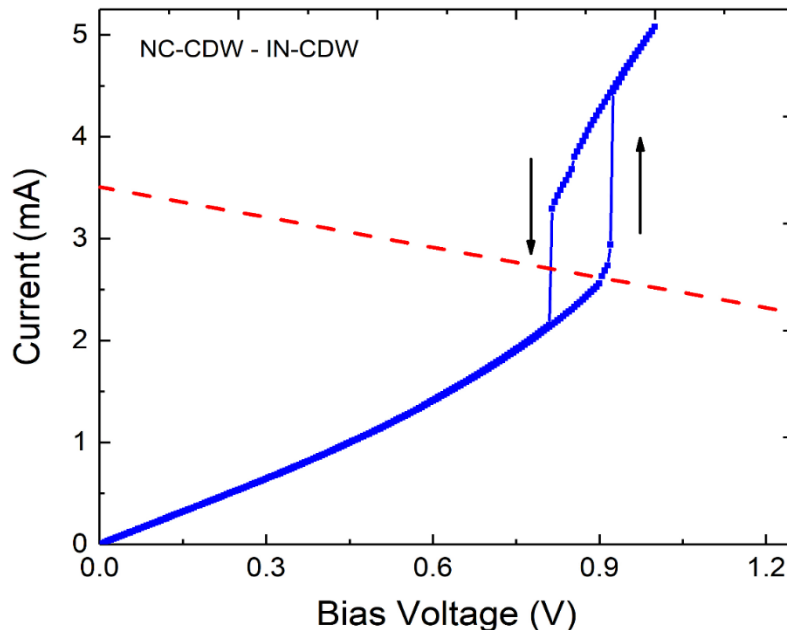


Frequency, f_0 of the noise peaks as a function of the current through 1T-TaS₂ device channel. The inset shows a microscopy image of a representative 1T-TaS₂ device structure with several metal contacts.



Relation between the COW current and fundamental oscillation frequency in NbSe₃. The inset shows I_{CDW}/f_0 vs. temperature. After Bardeen et al. (1982).

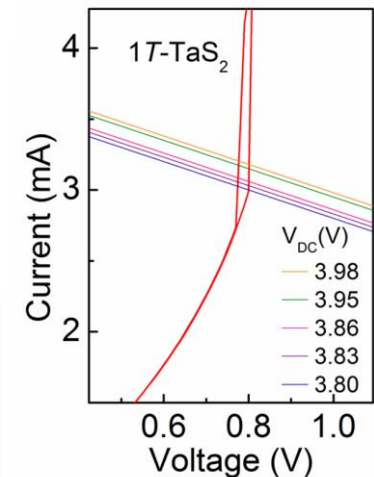
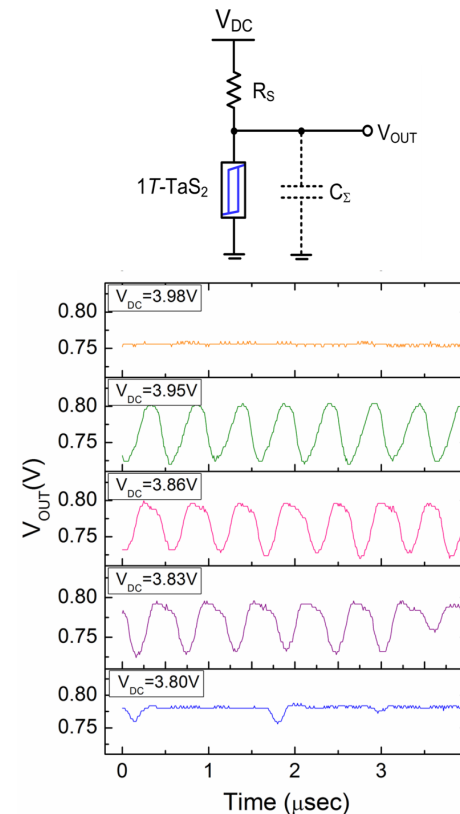
The Current Oscillations are due to Hysteresis at the NC-CDW – IC-CDW Transition



I-Vs of tested 1T-TaS₂ device which revealed “narrow band noise”. The hysteresis loop at the bias voltage $V = 0.9$ V corresponds to the transition from the NC-CDW phase to the IC-CDW phase induced by the applied electric field.

Adane K. Geremew, Sergey Rumyantsev, Roger Lake, Alexander A. Balandin, arXiv:2003.00356 (2020)

The current oscillations appear to be similar to our earlier result – this is not the “narrow band noise.”



G. Liu, B. Debnath, T. R. Pope, T. T. Salguero, R. K. Lake, and A. A. Balandin, Nature Nano, 11, 845 (2016).

Thank you – Questions?

